Genetic Algorithm Application to Enlarge Travel Range for Multi-Electrode MEMS Resonators

Yu Tian, Ronald N Miles, Shahrzad Towfighian
Department of Mechanical Engineering, Binghamton University, Binghamton, USA
stowfigh@binghamton.edu
0000-0002-5084-7395

Abstract—**While repulsive MEMS resonators overcome the pull-in collapse and achieve large strokes, they require high applied side voltages because they are based on the fringe-field effect in electrostatics. This paper uses the boundary element approach and a genetic algorithm to enlarge the travel range for the multi-electrode design. The enlargement is made possible by optimizing the dimensional parameters in the multi-electrode system that complies with PolyMUMPs fabrication technique. Compared with the results of the previous design, experimental measurements of the optimized dimensional parameters reveal up to 200% improvement in travel ranges. The effective method provides insight into more efficient generations of repulsive MEMS sensors and actuators.**

Index Terms—**electrostatic MEMS, repulsive actuation, resonator, boundary element approach, genetic algorithm, signal-to-noise ratio.**

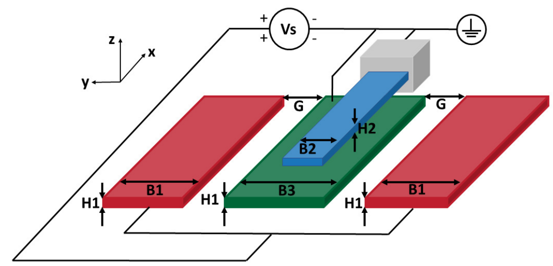

Fig. 1. Electrode arrangement of the repulsive resonator: cantilever beam (blue), anchor (gray), fixed center electrode (green), and fixed side electrodes (red). Dimensional parameters are indicated.

I. Introduction

Resonators have been broadly employed in applications of microelectromechanical systems (MEMS), including signal processing [1] and filtering [2], [3], energy harvesting [4], and many sensing scenarios [5]–[10]. They take advantage of micro structures that can be actuated at or close to the resonant frequencies to achieve speedy responses and very high signal-to-noise ratios. Among the MEMS mechanisms achieving resonant behaviors, electrostatic actuation has received significant attention because of several advantages: high compatibility with voltage sources in IC processes, low costs in bulk fabrication, and small power consumption.

The most popular technique for electrostatic resonators has been using two electrodes acting like parallel plates. They consist of a movable electrode, such as a micro beam, which is pulled into the fixed electrode. However, due to the pull-in instability problem, the movements can only be controlled in no more than one-third of the initial gap. Such a small distance as the travel range limits resonant behaviors for electrostatic resonators; therefore, the signal-to-noise ratios are significantly constrained. With the multi-electrode repulsive design introduced by S. He et al. [11], as shown in Fig. 1, two more fixed electrodes are charged with Vs and placed on both sides of the grounded parallel electrodes. This configuration generates a net electrostatic force that pushes the movable structure away from the substrate. Extensive simulations and experiments [12], [13] have shown that the pull-in instability no longer restricts the movable structure with repulsive actuation, and the travel range is improved by an order of the magnitude. Researchers have developed various repulsive resonators to pursue high signal-to-noise ratios and high sensitivities and resolutions in many applications [14]–[17]. Because the repulsive forces are relatively weaker than the attractive forces in the previous parallel plate design, especially when the resonator is vibrating far from the substrate, large travel ranges often require large side voltages Vs applied. This often causes additional problems with noise and safety.

For the multi-electrode design in the repulsive actuation, researchers have studied with finite element analysis method and found that manually tuning dimensional parameters based on experience has significant effects on increasing the travel range at moderate voltage Vs applied. These parameters include the widths and thicknesses of the electrodes and the lateral distance of the fixed electrodes in the arrangement in Fig. 1. Our paper explored the possibility of enlarging the travel range by searching for the global optimal dimensional parameters applying a genetic algorithm. This optimization method integrates the boundary element approach to efficiently approximate the electrostatic forces for the nonlinear multi-electrode configuration, a static solver to obtain the travel range for dimensional parameters, and a genetic algorithm to adjust and update the dimensional parameters to enlarge the travel ranges. Experiments of statics and dynamics in fundamental resonance are designed to demonstrate the improved travel ranges for the repulsive resonators.

The authors would like to acknowledge the financial support of the National Science Foundation (NSF) through Grant #1919608.

2022 IEEE Sensors | 978-1-6654-8464-0/22/$31.00 ©2022 IEEE | DOI: 10.1109/SENSORS52175.2022.9967334

Authorized licensed use limited to: STATE UNIV NY BINGHAMTON. Downloaded on March 29,2023 at 17:46:39 UTC from IEEE Xplore. Restrictions apply.

II. Method

The electrode arrangement of the repulsive resonator is composed of multiple electrodes, and their dimensional parameters are nonlinearly coupled to generate the electric field. It differs from parallel plate design, where the electric force is analytically derived. Therefore, we apply the boundary element approach to help determine the electric force from this multi-electrode configuration. The boundary element approach (BEA) is popularly used in estimating the capacitance in various acoustic sensors with complicated electrode arrangements [18]. In the boundary element approach, we first establish a 2D figure of the y-z cross-section of our four charged or grounded electrodes. The boundaries of these cross-sections are discretized to many line segments of finite length L_i. From electromagnetic theory, the electric potential v_i on each element L_i results from all elements (including itself) and is given by

$$v_i = \sum_j G_{ij} q_j = \sum_j C_{ij}^{-1} q_j \tag{1}$$

where C_{ij} is the corresponding element in the capacitance matrix representing the effect between $L_i - L_j$ pair, and G_{ij} is the inverse of the capacitance matrix. The total potential energy of the system is calculated using

$$Energy = \frac{1}{2}[q]^T[v] = \frac{1}{2}[v]^T[C][v] \tag{2}$$

with capacitance from BEA and known applied voltages (electric potentials) in electrostatic actuation. And the electric force is the gradient of the energy in the z-direction. After obtaining the net electric force from equation (2), the static deflection of the beam at a specific side voltage Vs is solved by a static solver based on the Bernoulli-Euler beam theory. Because there is an initial gap of 2 microns, the travel range allowing dynamic amplitudes at this voltage should be the summation of the static deflection and the initial gap.

The subsequent genetic algorithm uses the travel range as the cost function, and is applied to update the dimensional parameters listed in Table-I to maximize the travel range at our concerning voltages. Meanwhile, the dimensional parameters should always be constrained within the required ranges or of exact values to ensure successful fabrication. It is necessary to mention that we use a minimal varying range for the width of the beam because we don't want the natural frequency of our resonator to be shifted a lot. This is often an essential requirement in optimizing MEMS resonators that work for specific frequency ranges.

As the flowchart of the genetic algorithm in Fig. 2, several sets of variables are initially created. Taking advantage of the boundary element approach, the repulsive force generated by each set is modeled, and the travel range is computed. The travel ranges are sorted from least to most, and the best sets with the largest travel ranges are selected as sets of parents. The parents will generate potentially better sets by a series of genetic operators: crossover, mutation, and merge. These new sets are modeled with BEA again to verify if they have even more extensive travel ranges. The enlargement

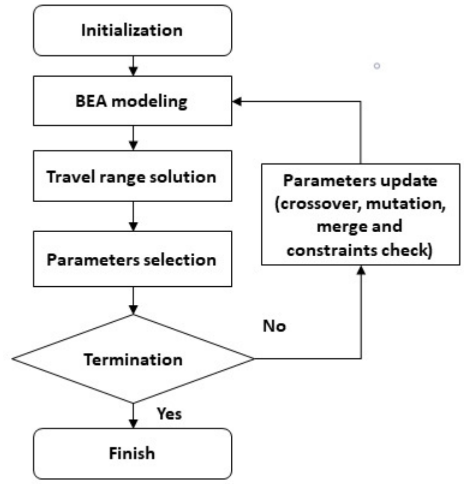

Fig. 2. Flowchart of the genetic algorithm.

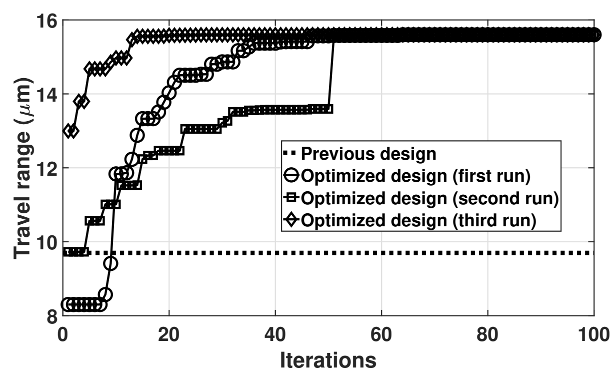

Fig. 3. Records of iterations corresponding to the largest travel range. Dotted line represents the travel range of the previous design and solid lines with markers represent three optimization runs for the same dimensional parameters of the optimized design.

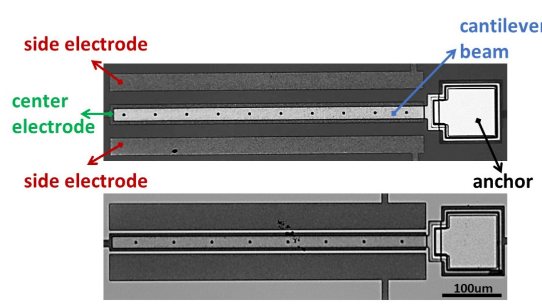

Fig. 4. Microscopic view of repulsive MEMS resonators: previous design (upper) and optimized design (lower). Multi-electrode arrangement is indicated.

Authorized licensed use limited to: STATE UNIV NY BINGHAMTON. Downloaded on March 29,2023 at 17:46:39 UTC from IEEE Xplore. Restrictions apply.

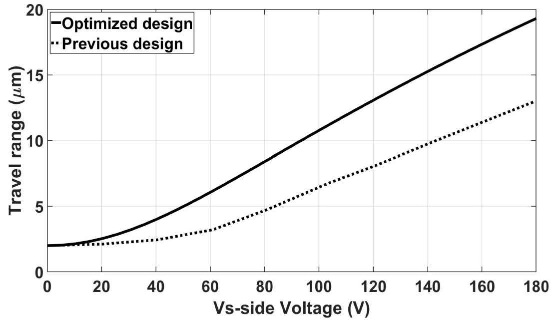

Fig. 5. Travel range obtained based on static measurements using a laser doppler vibrometer.

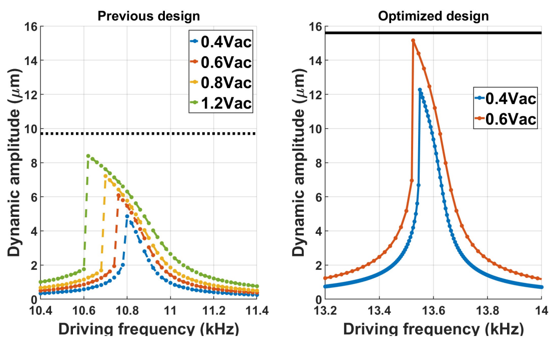

Fig. 6. Fundamental resonance at Vs=140+Vac*cos(2πft) and an air pressure Pa=1 torr. Black lines indicate the travel range of the previous resonator (dotted) and the optimized resonator (solid). Colored lines with circles indicate various levels of the applied AC voltage.

with a genetic algorithm is finished with up to 100 iterations, but usually, the best set is achieved convergently within 60 iterations, as shown in Fig. 3. The enlargement repeats for multiple concerning voltages (20V, 40V, ..., 180V), and the best sets establish an identical optimized design in Table-I. The optimized dimensional parameters maximize the size of side electrodes and minimize the dimensions of all other structures, including the width of the beam.

III. Results and Discussion

MEMSCAP fabricated the repulsive resonator of the optimized design following the PolyMUMPs standard process. One can find the comparison of the previous and the optimized design in microscopic views in Fig. 4. As it is shown, the optimized design is more compact than the previous design. A Polytec MSA-500 laser vibrometer was used to measure the static deflection and the dynamic displacement at the tip of the beam. The basic principle of laser vibrometer is the Doppler effect which relates the velocities of the moving object to the frequency changes detected by a high-precision interferometer. The displacement information can be attained by counting the light/dark fringes on the detector, and some techniques, including interpolation and digital demodulation, can help the vibrometer achieve excellent resolution in displacement measurement. The measured data were recorded and processed through a data acquisition system surrounding NI USB 6366

TABLE I
Dimensional parameters of MEMS resonators and constraints (Unit: μm)

Parameter	Constraints	Previous design	Optimized design
Side electrodes width	$10<B_1<38$	28	38
Cantilever width	$17.5\leq B_2\leq 20.5$	17.5	20.5
Middle electrodes width difference	$8<B_3-B_2<13$	12.5	8
Fixed electrodes gap	$4<G<21$	20.75	4
Fixed electrodes thickness	$H_1=0.5$	0.5	0.5
Cantilever thickness	$H_1=2$	2	2
Cantilever length	$L=500$	500	500

DAQ. Measurements of static deflection of the beams have demonstrated that the optimized design can achieve enlarged static deflections with an improvement from 64% to 200%. Added to the initial gap, the travel ranges allowing dynamic amplitudes for previous and optimized designs are shown in Fig. 5. This result also suggests that we can use much lower applied side voltages Vs to accommodate the same level of dynamic behaviors.

Fundamental resonance is the most popular scenario for repulsive MEMS resonators used as sensors and actuators. In the past, to accommodate a moderate level of the fundamental resonant amplitudes, applied voltages as high as 190V were often needed to have an extensive travel range available [14]. From the experiment-based dynamic amplitudes of the previous design and the optimized design in Fig. 6, with the same applied side voltage at 140V, the optimized design successfully holds a 60% increase in the resonant peak. The signal-to-noise ratio here is, therefore, significantly improved. It is valuable to mention that, with the travel range enlarged by the optimized dimensional parameters, the repulsive actuation is enhanced significantly. Applying an AC voltage of 0.6V, the optimized design travels to 16μm, while the amplitude of the previous design did not exceed 6μm. The proposed actuator design can be incorporated into levers used for MEMS mirrors to enhance their strokes.

IV. Conclusion

The contribution of this work is bridging the boundary element approach and a genetic algorithm to an efficient optimization strategy in MEMS resonators. The boundary element approach provides a platform to model the electrostatic field for a multi-electrode scheme. The travel ranges of the resonators are solved using an Euler-Bernoulli beam equation. A genetic algorithm updates the parameters to maximize the travel range. Because of the nonlinearity of the multi-electrode repulsive actuation, the optimal design can never be efficiently obtained with the empirical adjustments. Experiment-based comparisons show over 60% enlarged travel ranges, and much higher resonant peaks with lower applied AC voltages. This application can help researchers determine the optimized design of the multi-electrode MEMS devices, including but not limited to repulsive actuators.

Authorized licensed use limited to: STATE UNIV NY BINGHAMTON. Downloaded on March 29,2023 at 17:46:39 UTC from IEEE Xplore. Restrictions apply.

REFERENCES

[1] Zalalutdinov, M. K., Cross, J. D., Baldwin, J. W., Ilic, B. R., Zhou, W., Houston, B. H., and Parpia, J. M., 2010. "Cmos-integrated rf mems resonators". *Journal of Microelectromechanical Systems,* ***19***(4), pp. 807–815.

[2] Huang, F., Fouladi, S., and Mansour, R. R., 2011. "High-*q* tunable dielectric resonator filters using mems technology". *IEEE transactions on microwave theory and techniques,* ***59***(12), pp. 3401–3409.

[3] Pallay, M., Miles, R. N., and Towfighian, S., 2021. "Towards a high bias voltage mems filter using electrostatic levitation". *Mechanical Systems and Signal Processing,* ***150***, p. 107250.

[4] Ab Rahim, R., and bin Johari, M. J., 2016. "Design and simulation of mems helmholtz resonator for acoustic energy harvester". In 2016 International Conference on Computer and Communication Engineering (ICCCE), IEEE, pp. 505–510.

[5] Jha, C., Bahl, G., Melamud, R., Chandorkar, S., Hopcroft, M., Kim, B., Agarwal, M., Salvia, J., Mehta, H., and Kenny, T., 2007. "Cmos-compatible dual-resonator mems temperature sensor with milli-degree accuracy". In TRANSDUCERS 2007-2007 International Solid-State Sensors, Actuators and Microsystems Conference, IEEE, pp. 229–232.

[6] Pachkawade, V., 2021. "State-of-the-art in mode-localized mems coupled resonant sensors: A comprehensive review". *IEEE Sensors Journal*.

[7] Prud'Homme, A., and Nabki, F., 2020. "An 8 mw fully integrated regenerative resonant mems co 2 sensor using linear polyethylenimine as a capture layer". *IEEE Sensors Journal,* ***21***(5), pp. 5904–5913.

[8] Mousavi, M., Alzgool, M., and Towfighian, S., 2021. "A mems pressure sensor using electrostatic levitation". *IEEE Sensors Journal,* ***21***(17), pp. 18601–18608.

[9] He, S., and Mrad, R. B., 2004. "A novel mems tunable capacitor". In 2004 International Conference on MEMS, NANO and Smart Systems (ICMENS'04), pp. 618–622.

[10] Zamanzadeh, M., Jafarsadeghi-Pournaki, I., and Ouakad, H. M., 2020. "A resonant pressure mems sensor based on levitation force excitation detection". *Nonlinear Dynamics,* ***100***(2), pp. 1105–1123.

[11] He, S., and Mrad, R. B., 2008. "Design, modeling, and demonstration of a mems repulsive-force out-of-plane electrostatic micro actuator". *Journal of Microelectromechanical Systems,* ***17***(3), pp. 532–547.

[12] Daeichin, M., Miles, R. N., and Towfighian, S., 2021. "Large-stroke capacitive mems accelerometer without pull-in". *IEEE Sensors Journal,* ***21***(3), pp. 3097–3106.

[13] Ozdogan, M., Towfighian, S., and Miles, R. N., 2020. "Modeling and characterization of a pull-in free mems microphone". *IEEE Sensors Journal,* ***20***(12), pp. 6314–6323.

[14] Pallay, M., Daeichin, M., and Towfighian, S., 2017. "Dynamic behavior of an electrostatic mems resonator with repulsive actuation". *Nonlinear Dynamics,* ***89***(2), pp. 1525–1538.

[15] Pallay, M., and Towfighian, S., 2018. "A parametric electrostatic resonator using repulsive force". *Sensors and Actuators A: Physical,* ***277***, pp. 134–141.

[16] Tian, Y., Daeichin, M., and Towfighian, S., 2022. "Dynamic behavior of t-beam resonator with repulsive actuation". *Nonlinear Dynamics,* ***107***(1), pp. 15–31.

[17] Chong, J., He, S., and Ben Mrad, R., 2010. "Control of a surface micromachined repulsive-force driven 2d micromirror". In 2010 IEEE/ASME International Conference on Advanced Intelligent Mechatronics, pp. 1005–1007.

[18] Miles, R. N., 2020. "Estimation of capacitance". In *Physical Approach to Engineering Acoustics*. Springer, pp. 307–329.

Authorized licensed use limited to: STATE UNIV NY BINGHAMTON. Downloaded on March 29,2023 at 17:46:39 UTC from IEEE Xplore. Restrictions apply.